Quantifying rock uplift rates using channel steepness and cosmogenic nuclide–determined erosion rates: Examples from northern and southern Italy

Andrew J. Cyr[1,†], Darryl E. Granger[1], Valerio Olivetti[2], and Paola Molin[2]
[1]DEPARTMENT OF EARTH AND ATMOSPHERIC SCIENCES, PURDUE UNIVERSITY, 550 STADIUM MALL DRIVE, WEST LAFAYETTE, INDIANA 47907, USA
[2]DIPARTIMENTO DI SCIENZE GEOLOGICHE, UNIVERSITÀ DEGLI STUDI "ROMA TRE," LARGO SAN LEONARDO MURIALDO 1, 00146 ROME, ITALY

ABSTRACT

Rock uplift rates can be difficult to measure over 10^3–10^5 yr time scales. If, however, a landscape approaches steady state, where hillslope erosion and rock uplift rates are steady and locally similar, then it should be possible to quantify rock uplift rates from hillslope erosion rates. Here, we test this prediction by comparing channel steepness index values and ^{10}Be catchment-averaged erosion rates to well-constrained rock uplift rates in two landscapes in Italy. The first field area is the Romagna Apennines, northern Italy, where rock uplift rates are relatively uniform, between 0.2 and 0.5 mm/yr (regional mean 0.40 ± 0.15 [SE] mm/yr), and have been steady since 0.9 Ma. The second area is the region around northeastern Sicily and the southernmost Italian peninsula, where rock uplift rates are higher and exhibit a strong spatial gradient, from ~0.7 to ~1.6 mm/yr (regional mean 1.09 ± 0.13 [SE] mm/yr). In both regions, channel steepness indices and ^{10}Be erosion rates vary directly with rock uplift rates. Although there is considerable variability in erosion rates, regionally averaged rates in both the northern (0.46 ± 0.04 [SE] mm/yr) and southern (1.21 ± 0.24 [SE] mm/yr) areas accurately measure rock uplift rates. Although channel steepness indices do not quantify rock uplift rates, they are useful for (1) identifying regional patterns of rock uplift, (2) identifying areas where uplift rates might be expected to be uniform, and (3) informing ^{10}Be sampling strategies. This study demonstrates that, together, channel steepness and hillslope erosion rates can provide a powerful tool for determining rock uplift rates.

LITHOSPHERE; v. 2; no. 3; p. 188–198, Data Repository 2010137. doi: 10.1130/L96.1

INTRODUCTION

Knowing the distribution of rock uplift rates across a landscape is important for identifying and understanding active tectonic structures, and for establishing the pace and pattern of mountain growth. Rock uplift rates can be determined geodetically over short (10^0–10^2 yr) time scales, or inferred from thermochronometers over much longer (10^6 yr) time scales. Over intermediate (10^3–10^5 yr) time scales, rock uplift rates can be inferred from uplifted geomorphic markers such as marine or fluvial terraces, provided that their ages can be determined. Each of these methods provides important constraints but also suffers from limitations. Geodetic measurements only incorporate a fraction of the seismic cycle and are limited to sites with existing surveys and where uplift rates are rapid enough to be measured precisely. Thermochronology indicates the time taken to exhume rocks by kilometers and cannot typically resolve shorter-term patterns. Uplifted fluvial strath terraces require the assumption that river incision is equilibrated with rock uplift, yet strath formation is often attributed to climatic fluctuations, making it difficult to distinguish climatic from tectonic causes of river incision (e.g., Pazzaglia and Gardner, 1993; Merritts et al., 1994; Hancock et al., 1999; Wegmann and Pazzaglia, 2002; Pan et al., 2003).

Alternative methods for inferring local- to regional-scale rock uplift rates, such as stream-channel morphometry and catchment-averaged erosion rates, have become increasingly used to measure relative differences in rock uplift rates across a region (Lague et al., 2000; Kirby and Whipple, 2001; Kobor and Roering, 2004; Ferrier et al., 2005; Wobus et al., 2005, 2006; Kirby et al., 2007). These methods are widely applicable; however, they implicitly assume a landscape in steady state or dynamic equilibrium, in which erosion and river incision are equal to rock uplift. This assumption is difficult to test. Nevertheless, both channel steepness index, a proxy for river incision rate, and cosmogenic nuclide–determined erosion rates have become widely used with at least qualitative success. What remains to be demonstrated is a quantitative test of both channel steepness index and erosion rate as indicators of rock uplift rates in a place where uplift rates are known independently.

In the following section, we briefly introduce the use of channel steepness index and erosion rate to determine rock uplift rates, with an emphasis on the assumptions and conditions necessary for their success. Channel steepness index is a measure of stream-channel gradient normalized to drainage area (see Wobus et al., 2006), and it has been shown to be directly proportional to rock uplift rates in a variety of landscapes (e.g., Snyder et al., 2000; Lague and Davy, 2003; Duvall et al., 2004). We measured erosion rates using cosmogenic ^{10}Be in quartz, which is produced in proportion to the residence time of mineral grains in the uppermost few meters of Earth's surface. We then applied both of these methods to two different landscapes in Italy, where rock uplift rates are known independently from marine terrace stratigraphy.

Channel Steepness Index

Bedrock river channel steepness index can be used to infer relative differences in rock uplift rates across a landscape, given uniform lithology and climatic forcing. River incision, E, is

†Present address: U.S. Geological Survey, 345 Middlefield Road, Menlo Park, California 94025, USA; e-mail: acyr@usgs.gov.

often cast as a function of basal shear stress, and can be expressed as (Howard and Kerby, 1983; Howard et al., 1994),

$$E = KA^m S^n, \quad (1)$$

where S is local channel slope, A is the contributing drainage area that serves as a proxy for local discharge, K is a variable that incorporates incision process–, substrate-, climate-, and hydrology-dependent variables (see Whipple, 2004), and m and n are positive constants that are functions of basin hydrology, channel geometry, and specific incision process (Howard et al., 1994; Whipple and Tucker, 1999; Whipple et al., 2000a).

The change in channel bed elevation at any point along the longitudinal profile with respect to time, dz/dt, reflects a competition between the rates of rock uplift and channel incision with respect to base level. This can be expressed as,

$$dz/dt = U - E = U - KA^m S^n, \quad (2)$$

where U is the rock uplift rate. For a steady-state landscape, where river incision rate is equal to the rock uplift rate, $dz/dt = 0$, and Equation 2 can be solved for equilibrium channel slope, S, at a given drainage area, A,

$$S = k_s A^{-\theta}, \quad (3a)$$

where k_s describes the channel steepness, and θ describes the channel concavity (the rate of change of local channel slope as a function of increasing drainage area; Hack, 1957; Flint, 1974; Tarboton et al., 1989). The coefficient k_s and the exponent θ are referred to as the channel steepness index and channel concavity index, respectively (Snyder et al., 2000). The channel steepness index, k_s, is in turn a function of both rock uplift rate, U, and rock resistance to erosion, K, which is a variable that incorporates both process- and substrate-dependent variables (see Whipple, 2004), according to

$$k_s = (U/K)^{1/n}, \quad (3b)$$

$$\theta = m/n. \quad (3c)$$

The exponent n, which remains poorly constrained, relates incision rate to channel slope and is typically assigned a value of 2/3 (Howard and Kerby, 1983), 1 (Stock and Montgomery, 1999), or somewhere between 0.2 and 0.6 (Whipple et al., 2000b). Moreover, both m and n may or may not be process dependent (Whipple et al., 2000b; Hancock et al., 1998). However, regardless of the specific values of m and n, based on theoretical (Whipple and Tucker, 1999) and empirical (Howard and Kerby, 1983; Tarboton et al., 1991; Snyder et al., 2000) arguments, their ratio (θ) should be between 0.35 and 0.6.

Channel steepness index can be obtained by either surveying stream channels or by regression of local channel slopes and drainage areas obtained from digital elevation models (e.g., Wobus et al., 2006). Provided that K and n are uniform across the region of interest, then variations in k_s among channels or channel segments will track variations in uplift rate (Whipple and Tucker, 1999; Snyder et al., 2000). It is difficult to solve for rock uplift rates directly, because K is poorly constrained. For example, Stock and Montgomery (1999) suggested that K may vary over several orders of magnitude due to spatial differences in rock properties, as well as due to the frequency of discharge events significant enough to initiate bedrock incision. Additionally, in order for k_s to indicate relative changes in rock uplift rates, the channel longitudinal profile must be in steady state and reflect the current climatic and tectonic conditions. Both U and K must be uniform along the entire channel length.

Empirical support for a correlation between channel steepness index and rock uplift rates is emerging from multiple landscapes around the globe. In two regions of coastal California, Snyder et al. (2000), working in the King Range, and Duvall et al. (2004), working in the Santa Ynez Range, found that the steepness index values of small bedrock channels were higher at higher rock uplift rates as inferred from the elevations of marine terraces (Merritts and Bull, 1989; Metcalf, 1994; Gurrola et al., 1998; Trecker et al., 1998). Multiple studies have demonstrated a similar relationship in the Siwalik Hills of central Nepal (Kirby and Whipple, 2001; Lague and Davy, 2003; Wobus et al., 2006) and in the northern Apennines, Italy (Wilson et al., 2009), where systematic changes in steepness index have been correlated with rock uplift rate across a fault-bend fold (Lavé and Avouac, 2001) and a fault-propagation fold (Wilson et al., 2009), respectively.

Erosion Rates

It is commonly assumed that over tectonogeomorphic time scales (10^4–10^6 yr), landscapes approach a condition of dynamic equilibrium, in which erosion and river incision rates roughly balance rock uplift rates (e.g., Hack, 1960; Schumm and Lichty, 1965). A perfect match between rock uplift and erosion may never be achieved, because erosion rates will vary with climate change (e.g., Whipple et al., 1999). Nevertheless, isostasy alone dictates that in compensated orogens, erosion drives at least ~80% of rock uplift, and in an orogen maintaining a constant elevation, erosion must equal rock uplift (Molnar and England, 1990). In these cases, a measure of spatially averaged erosion rates over time scales of 10^3 to 10^5 yr should closely correspond to the regionally averaged rock uplift rate.

Spatially averaged erosion rates can be estimated using cosmogenic nuclides such as ^{10}Be in quartz-bearing alluvial sediment (Brown et al., 1995; Bierman and Steig, 1996; Granger et al., 1996). Beryllium-10 accumulates in quartz near Earth's surface proportional to its local production rate and inversely proportional to the surface erosion rate. The cosmogenic nuclide method averages erosion rates over the time required to erode a catchment by about one secondary cosmic-ray penetration length, or ~60 cm in rock of density 2.6 g/cm^3 (Masarik and Reedy, 1995). In most landscapes, this is anywhere from 10^3 to 10^5 yr.

Several conditions must be met for cosmogenic nuclides to accurately indicate catchment-averaged erosion rates. Quartz must be distributed evenly throughout the catchment, or else erosion rates will be biased to areas of higher quartz content. Sediment samples must be representative of the entire watershed, rather than be dominated by a single landslide. If erosion occurs primarily by landsliding, then the watershed should be large enough that a sediment sample is likely to contain grains from many different landslides (Niemi et al., 2005; Yanites et al., 2009). The catchment should not be glaciated, since glaciation may disrupt sediment transport paths, making stream sediment unrepresentative of the catchment as a whole (von Blanckenburg, 2005; Wittmann et al., 2007; Stock et al., 2009). Finally, erosion must occur at a nearly constant rate over the time taken to erode several secondary cosmic-ray penetration lengths (a few meters). If erosion rates change through time, cosmogenic nuclide concentrations will provide an average erosion rate (Schaller and Ehlers, 2006).

Empirical data from a variety of landscapes suggest a correlation between cosmogenic nuclide–determined erosion rates and rock uplift inferred by different methods. In both tectonically quiescent and tectonically active mountain ranges, cosmogenic nuclide–determined, millennial erosion rates are similar to longer-term (10^6 yr) exhumation rates as inferred from low-temperature thermochronometry (e.g., Kirchner et al., 2001; Matmon et al., 2003; Vance et al., 2003; Safran et al., 2005; Stock et al., 2009). Although rock exhumation does not necessarily equal rock uplift, these results are compelling when considered in the context of two recent studies in which cosmogenic nuclide erosion

rates were compared directly to uplift rates determined by geodetic methods. Wittmann et al. (2007) and Champagnac et al. (2009) documented erosion rates in the Swiss central Alps that were locally similar to decadal-scale uplift rates determined by Global Positioning System (GPS) and re-leveling. In a similar study in the northern and central Apennines, Italy, erosion rates were similar to both short-term rock uplift determined by geodetic methods and long-term (10^5 yr) rock uplift rates determined from marine deposits and fluvial terrace stratigraphy (Cyr and Granger, 2008). On the other hand, Ferrier et al. (2005) found that two catchments on the northern California coast are eroding substantially slower than uplift rates and river incision rates determined from marine terraces, indicating an increasing mean elevation across the area or that erosion by landslides is underrepresented. While these studies suggest that erosion rates may equal rock uplift rates, at least in some settings, a test of the sensitivity of erosion rates to a wide range of independently determined, long-term rock uplift rates has yet to be performed.

STUDY AREAS

To test the accuracy and sensitivity of bedrock channel steepness index and catchment-averaged erosion rates as indicators of rock uplift rates, we chose two landscapes in Italy (Fig. 1) where rock uplift rates are known from marine and fluvial terrace stratigraphy. The Romagna Apennines, northern Italy, have relatively low and uniform rock uplift rates (Cyr and Granger, 2008; Picotti and Pazzaglia, 2008; Wegmann and Pazzaglia, 2009), whereas the Peloritani Mountains, northeastern Sicily, and the Aspromonte Massif, southern Italy, have higher and spatially variable rock uplift rates (Cosentino and Gliozzi, 1988; Miayuchi et al., 1994; Bordoni and Valensise, 1998; Ferranti et al., 2006).

Romagna Apennines

The Romagna Apennines have developed as a result of collision between the Adriatic promontory of the African plate and the southern margin of the European plate. They emerged above sea level ca. 4 Ma after the northern Apennines accretionary wedge overrode thicker, more buoyant Adriatic continental crust (Castellarin et al., 1985; Ricci-Lucchi, 1986; Zattin et al., 2002; Bartolini, 2003; Picotti and Pazzaglia, 2008). Presently, the Romagna Apennines expose a Miocene-aged, uniform sequence of quartz-rich, shaly-arenaceous sandstone (Ricci Lucchi, 1986; Zattin et al., 2000; Feroni et al., 2001). River channels have either bedrock or mixed alluvial-bedrock cover (Simoni et al., 2003; Spagnolo and Pazzaglia, 2005), indicating that channel incision is likely detachment-limited. Hillslopes in the Romagna Apennines are mantled by thin (<1 m) soil (Simoni et al., 2003; Spagnolo and Pazzaglia, 2005) and hillslope erosion is dominated by shallow landsliding (Simoni et al., 2003; Del Maschio et al., 2005).

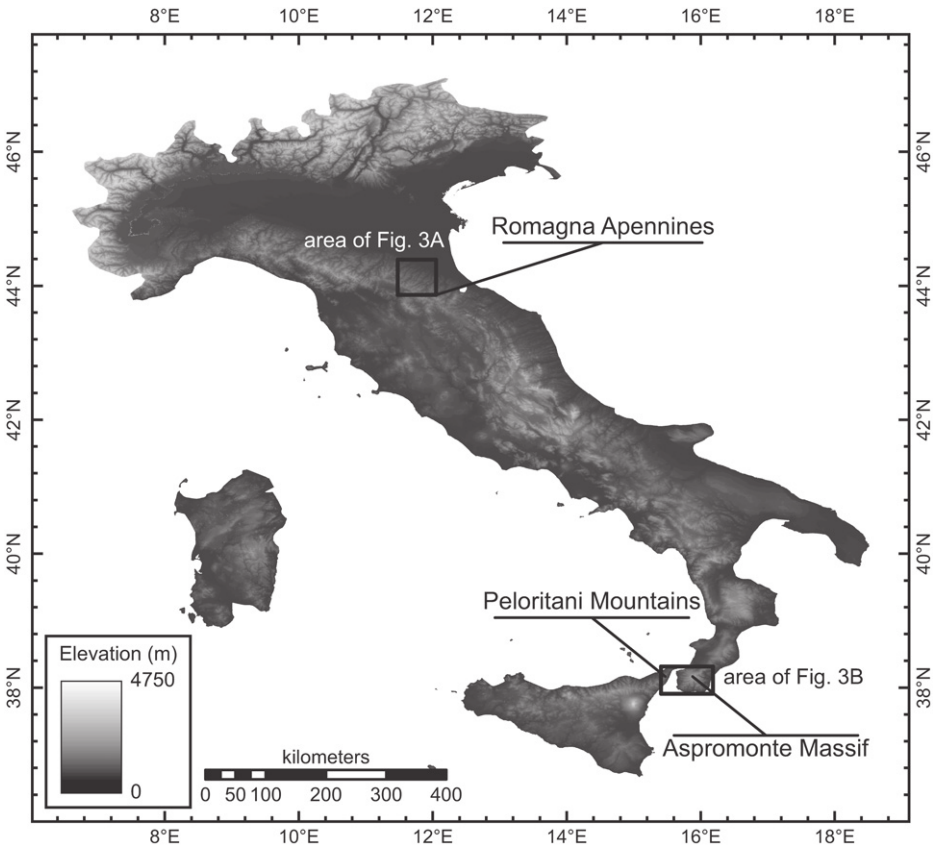

Figure 1. Simplified map of Italy showing the locations of the Romagna Apennines, Peloritani Mountains, and Aspromonte Massif study areas. Elevations are SRTM 3 arc-second (~90 m) data.

Short- and long-term rock uplift rates in the Romagna Apennines have been constrained by a recent geodetic re-leveling survey and by marine deposit and fluvial terrace stratigraphy. D'Anastasio et al. (2006) used geodetic re-leveling of a network of benchmarks in place since 1870 to measure rock uplift rates within major river valleys and along the crest of the northern and central Apennines. Relative to a benchmark at Genoa (sea level), mean rock uplift rates in the Reno River valley, at the northern edge of the Romagna Apennines, are 1.0 ± 0.2 mm/yr, and those in the Marecchia valley, at the southern edge of the Romagna Apennines, are 0.41 ± 0.26 mm/yr since 1870. The stated uncertainties reflect the standard deviation of all D'Anastasio et al.'s (2006) uplift rate determinations along a given re-leveling transect. We refer the interested reader to D'Anastasio et al. (2006) for a detailed description of how they handled uncertainties in each re-leveling measurement. Higher rock uplift rates in the Reno River valley likely reflect actively growing structures at the mountain front (Picotti and Pazzaglia, 2008). Longer-term (10^3–10^5 yr) rock uplift rates can be inferred from the ages and elevations of uplifted fluvial-deltaic/nearshore deposits exposed along the northern and central Apennines mountain front, and from fluvial strath terrace stratigraphy upstream of the mountain front. Paleomagnetic, biostratigraphic, and electron spin resonance (ESR) data constrain the age of the Sabbie Gialle, an uplifted fluvial-deltaic/nearshore sequence of sandstones and mudstones exposed along the mountain front (Marabini et al., 1995) to between 0.78 and 1.0 Ma (Colalongo et al., 1979; Gagnepain et al., 1996; Falguères, 2003). Assuming a deposition age of ca. 0.9 Ma and the modern elevation of the Sabbie Gialle (200–300 m; Marabini et al., 1995), the rock uplift rate of the Romagna Apennines front since 0.9 Ma is between 0.22 and 0.36 mm/yr. Beginning ~3–5 km upstream of the mountain front, strath terraces in the Reno

River valley (Picotti and Pazzaglia, 2008), on the northern edge of the Romagna Apennines, and in the Bidente and Musone River valleys (Wegmann and Pazzaglia, 2009), on the southern edge of the study area, both dated using radiocarbon, indicate uplift rates between 0.2 and 0.5 mm/yr between 900 and 140 ka in the area where ^{10}Be samples were collected.

Peloritani Mountains and Aspromonte Massif

The Peloritani Mountains and Aspromonte Massif expose Mesozoic sedimentary cover rocks and late Paleozoic–aged quartzofeldspathic, crystalline igneous, and metamorphic rocks (Amodio-Morelli et al., 1976; Catalano and D'Argenio, 1978; Bonardi et al., 1980; Nigro, 1996) that were exhumed to within a few kilometers of the surface (temperatures between 250 °C and 70 °C) between ca. 35 and 15 Ma due to a combination of accelerated surface erosion (Thomson, 1994, 1998) and localized late-orogenic extension (Platt and Compagnoni, 1990). They attained their geographic position and elevation due to a pulse of rapid rock uplift during the late Pliocene to early Pleistocene (between 1.0 and 0.8 Ma), likely in response to a change in the axis of backarc spreading in the Tyrrhenian Sea (Hippolyte et al., 1994) and/or delamination and rollback of the subducting Ionian slab (Faccenna et al., 2001, 2004). These mountain ranges support a deeply dissected, generally high-relief landscape that has small patches of low-relief, relict landscape preserved at the highest elevations, generally greater than ~1800 m above sea level. These patches of relict landscape typically display deep weathering profiles, with saprolite between 5 and 10 m thick, mantled by organic soils (Ietto et al., 2007). The flanks of the Peloritani and Aspromonte are drained by small catchments characterized by steep channel and hillslope gradients (Le Pera and Sorriso-Valvo, 2000). Channels are floored by either bedrock or coarse sand– to cobble-sized sediment, but they are typically incising their beds and undercutting hillslopes (Le Pera and Sorriso-Valvo, 2000; Ietto et al., 2007). Hillslope erosion occurs primarily by shallow landsliding (Le Pera and Sorriso-Valvo, 2000; Ietto et al., 2007), although deep-seated bedrock landslides have been observed in the steepest upper reaches of some drainages during either heavy rainfall or large seismic events (Pellegrino and Prestininzi, 2007).

Long-term rock uplift rates in the Peloritani and Aspromonte are constrained by marine terraces, the most extensive of which have been attributed to the marine isotope stage (MIS) 5e highstand (ca. 125 ka) based on the presence of a unique and short-lived faunal assemblage, and radiometric and electron spin resonance ages (see Ferranti et al., 2006). Rock uplift rates vary spatially, with the highest rates of 1.63 mm/yr near the Messina Strait, decreasing to ~0.6 mm/yr at the eastern end of our study area (Cosentino and Gliozzi, 1988; Miayuchi et al., 1994; Bordoni and Valensise, 1998; Ferranti et al., 2006).

METHODS

Channel Morphologic Analysis

Channel longitudinal profiles were extracted from 3 arc-second (~90 m) shuttle radar topography mission (SRTM) data and analyzed in MatLab using the Stream Profiler codes developed by Snyder et al. (2000) and Kirby and Whipple (2001), and detailed in Wobus et al. (2006) and Whipple et al. (2007). These codes are publicly available at http://geomorphtools.org. Channel longitudinal profiles derived from SRTM data contain several segments with zero slope, which are the result of nonphysical artifacts in the SRTM data and the ArcGIS pit-filling routine. These artifacts mean that some smoothing of the original SRTM data must be applied. Channel profiles were smoothed using a moving window average of ~11 pixels (1000 m). This method effectively minimizes noise in the SRTM data while maintaining the form of the longitudinal profile. It has been shown that longitudinal profiles extracted from digital elevation data according to these methods are similar to profiles determined by digitizing topographic maps (e.g., Snyder et al., 2000) and from detailed surveys of channel elevations (e.g., Snyder et al., 2000; Kirby and Whipple, 2001). Local channel gradients were calculated over a constant vertical interval of 10 m from the smoothed elevation data (Snyder et al., 2000; Kirby and Whipple, 2001; Wobus et al., 2006), and linear regressions of these local channel slopes and their respective drainage areas in log-log space were used to determine the values of the channel concavity (θ, the slope of the regression) and channel steepness (k_s, the y-intercept of the regression) index values (Eq. 3). A recent review by Wobus et al. (2006) provides a detailed description of data handling and processing procedures, as well as analytical techniques.

Slope-area relationships described by Equation 3 are only valid for detachment-limited, bedrock fluvial channels. The transition from unchannelized headwaters or debris flow–dominated channels to those characterized by fluvial processes has been identified from digital elevation data by many workers (e.g., Dietrich et al., 1993; Montgomery and Foufoula-Georgiou, 1993; Stock and Dietrich, 2003; Wobus et al., 2006), where the slope-area data of unchannelized or debris flow–dominated reaches have local slopes that do not vary as a function of increasing drainage area. This transition is well defined in all of the catchments examined in the Romagna Apennines and Peloritani and Aspromonte, and it typically occurs in drainage areas between 1 and 10 km^2 (Fig. 2). It is likely that this is actually a gradual transition and that many upper reaches of our fluvial channels may periodically be better characterized by debris-flow processes (e.g., Stock and Dietrich, 1998); however, differences in channel longitudinal profile form along the observed spatial gradient in rock uplift rate are not likely to significantly alter these analyses (Kirby et al., 2007). Regressions of slope-area data were not extended beyond the downstream transition to alluvial-fan and coastal-plain deposits in the lower reaches of Romagna Apennines and Peloritani-Aspromonte rivers, respectively.

Direct comparisons of the k_s values of one channel to another can be problematic because of the autocorrelation between k_s and θ (e.g., Sklar and Dietrich, 1998). In order to compare the channel steepness index values of drainages that have different concavities, a normalized channel steepness index, k_{sn}, is calculated using a reference concavity, θ_{ref} (e.g., Snyder et al., 2000; Kirby et al., 2003; Wobus et al., 2006). Typically, θ_{ref} is taken as the mean of observed θ values in a given field area; however, relative differences in k_s should be maintained regardless of the specific choice of θ_{ref} (Wobus et al., 2006). We calculated k_{sn} values using $\theta_{ref} = 0.45$. While this θ_{ref} is different from the average concavities for the Romagna Apennines and Peloritani-Aspromonte (Table 1), it allows immediate direct comparisons to k_{sn} values determined in other studies (e.g., Snyder et al., 2003; Duvall et al., 2004; Wobus et al., 2006; Kirby et al., 2007; Ouimet et al., 2009) and does not change the results of our analysis (Table DR2; Fig. DR4).[1]

Erosion Rates

We calculated catchment-averaged erosion rates from cosmogenic ^{10}Be in quartz-bearing stream sediments (Brown et al., 1995; Bierman and Steig, 1996; Granger et al., 1996). Samples for ^{10}Be analysis were collected from either the active channels or overbank deposits of both main-stem and tributary channels of three catchments in the Romagna and five catchments in

[1]GSA Data Repository Item 2010137, Figures DR1–DR4 and Tables DR1–DR2, is available at www.geosociety.org/pubs/ft2010.htm, or on request from editing@geosociety.org, Documents Secretary, GSA, P.O. Box 9140, Boulder, CO 80301-9140, USA.

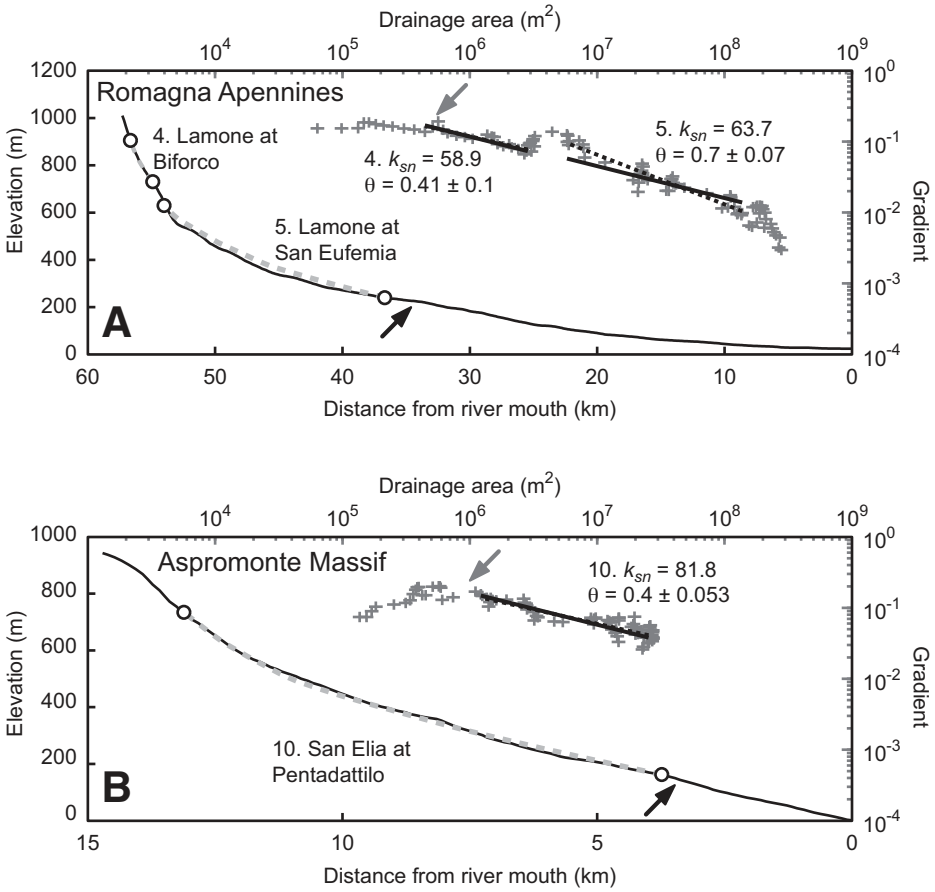

Figure 2. Examples of stream-channel longitudinal profiles (left and bottom axes) and slope-area data (top and right axes) from the Romagna Apennines (A) and Aspromonte Massif (B) used to determine k_{sn} values. Channel longitudinal profiles: black solid line—smoothed channel profile; gray dashed line—best-fit channel profile calculated from k_{sn} and best-fit θ, white circles—limits of channel data used in the regression. Slope/area data: gray crosses—log-binned slope-area data; dashed black line—best-fit slope-area regression; solid black line—slope-area regression using θ_{ref}. The black arrow denotes the mapped transition from detachment-limited to transport-limited channels. The gray arrows show the transition from channels dominated by unchannelized hillslope and/or debris-flow processes to those characterized by fluvial processes inferred from the slope-area relationships. Numbers before stream name and sample location correspond to those in Figure 3 and Tables 1 and 2.

the Peloritani and Aspromonte. Samples were collected from upstream of the mountain front in the Romagna Apennines, whereas in the Peloritani and Aspromonte, they were collected upstream of the observed downstream transition to completely alluviated channels. In addition to minimizing the potential for older fluvial sediments to affect cosmogenic ^{10}Be concentrations, this sampling strategy ensures that catchment-averaged erosion rates are being compared over the channel segments where k_{sn} values were calculated. Catchments upstream of sampling locations drain either a single, lithologically uniform formation (Romagna Apennines) or lithology (Peloritani and Aspromonte), which should minimize the effects of nonuniform quartz concentrations on our calculated erosion rates. In both regions, hillslope erosion is dominated by shallow landsliding; however, the sampled catchments are sufficiently large that landslide-derived sediment should be well mixed and representative of long-term catchment-wide erosion rates (Niemi et al., 2005; Yanites et al., 2009). Hillslope erosion rates calculated from the ^{10}Be concentrations of sediment from some catchments draining the Aspromonte Massif could potentially be biased by quartz enrichment in the soils and saprolite present on the relict landscape (Granger et al., 2001; Riebe et al., 2001). However, these areas are small and are not sampled by the selected drainage basins. The procedures used to physically separate quartz and chemically isolate ^{10}Be are detailed in Appendix DR1 (see footnote 1).

Erosion rates, ε, were calculated from the concentrations of ^{10}Be produced by both spallation reactions (the first term) and muogenic processes (the last three terms) according to

$$N = \frac{P_n}{\left(1/\tau + \rho\varepsilon/\Lambda\right)} + \frac{P_{\mu 1}}{\left(1/\tau + \rho\varepsilon/L_1\right)} + \frac{P_{\mu 2}}{\left(1/\tau + \rho\varepsilon/L_2\right)} + \frac{P_{\mu 3}}{\left(1/\tau + \rho\varepsilon/L_3\right)} \quad (4)$$

(Granger et al., 2001), where P_n, $P_{\mu 1}$, $P_{\mu 2}$, and $P_{\mu 3}$, are the production rates of ^{10}Be by spallation and muon processes, τ is the radioactive mean-life of ^{10}Be, ρ is the material density, Λ is the attenuation length for ^{10}Be production by spallation, and L_1, L_2, and L_3 are the attenuation lengths for ^{10}Be production by muon reactions. Local production rates of ^{10}Be were scaled from sea-level, high-latitude values given in Table DR1 (see footnote 1; Granger and Smith, 2000) according to Stone (2000), and using the area-weighted, catchment-averaged production rate. Snow depth records are not available for all of the examined catchments, and so we did not adjust local production rates for snow shielding.

RESULTS

Channel Morphometry

Normalized channel steepness index values were determined for seven channels in the Romagna Apennines, and five channels in the Peloritani and Aspromonte. The results of the channel morphologic analyses are presented in Table 1, Figure 3, and Figures DR1–DR3 (see footnote 1). Normalized channel steepness index values in the Romagna Apennines fall within a narrow range between 46.0 ± 1.0 and 63.7 ± 1.5 $m^{0.9}$, with a regional mean of 57.5 ± 2.4 (SE) $m^{0.9}$. Channel steepness values of the lower-elevation channel segments are slightly higher than higher-elevation segments, although the observed variability is not different from similar studies where rock uplift rates are uniform (e.g., Snyder et al., 2000; Duvall et al., 2004). In the Peloritani and Aspromonte, k_{sn} values are all higher than those in the Romagna Apennines, ranging from 75.3 ± 1.0 to 108.4 ± 5.4 $m^{0.9}$, with a regional mean of 97.6 ± 14.5 (SE) $m^{0.9}$, and increase in proportion to rock uplift rates (Figs. 3 and 4).

Cosmogenic Nuclides

Millennial-scale, catchment-averaged hillslope erosion rates determined from the ^{10}Be

TABLE 1. RESULTS OF MORPHOMETRIC ANALYSES IN THE ROMAGNA APENNINES, PELORITANI MOUNTAINS, AND CALABRIAN ARC

River (river at location)*	A_{min} (km^2)	A_{max} (km^2)	θ† (dS/dA)	k_{sn}§ ($m^{0.9}$)	Mean basin slope# (m/m)
Romagna Apennines					
1. Visano at Palazzuolo	1.12	8.81	0.42 ± 0.04	55.7 ± 0.5	0.358
2. Senio at Palazzuolo	1.12	17.37	0.56 ± 0.06	52.7 ± 1.4	0.346
3. Senio at Casola	1.12	114.41	0.64 ± 0.33	62.4 ± 1.3	0.349
4. Lamone at Biforco	1.47	44.28	0.41 ± 0.10	58.9 ± 0.7	0.370
5. Lamone at San Eufemia	1.47	114.41	0.70 ± 0.07	63.7 ± 1.5	0.348
6. Montone at San Benedetto	1.17	52.08	0.50 ± 0.11	46.0 ± 1.0	0.346
7. Montone at Davadola	1.17	183.46	0.65 ± 0.09	63.4 ± 2.0	0.321
Mean and 1 standard error**			**0.55 ± 0.04**	**57.5 ± 2.48**	
Peloritani Mountains					
8. Pagliara at Roccalumera	1.28	22.69	0.41 ± 0.04	75.3 ± 1.0	0.424
9. Fiumedinisi at Nizza di Sicilia	1.10	45.64	0.51 ± 0.04	85.4 ± 0.5	0.440
Aspromonte Massif					
10. San Elia at Pentedátillo	1.45	23.96	0.40 ± 0.05	81.8 ± 0.8	0.298
11. San Pasquale at Palizzi	1.85	18.48	1.10 ± 0.12	155.0 ± 5.4	0.337
12. Torno at Burzzano Zeffírio	1.01	34.28	0.59 ± 0.12	90.5 ± 11.5	0.294
Mean and 1 standard error			**0.60 ± 0.13**	**97.6 ± 14.5**	

*Location is name of the town nearest to where the sample was collected, according to the Millennial edition of *Atlante Stradale d'Italia* by the Touring Club Italiano.
†Best-fit channel concavity.
§Normalized channel steepness index calculated using $\theta_{ref} = 0.45$.
#Calculated using standard algorithms in the River Tools software package.
**Calculated as $(1\sigma/\sqrt{N})$, where σ is the standard deviation, and N is the number of data points.

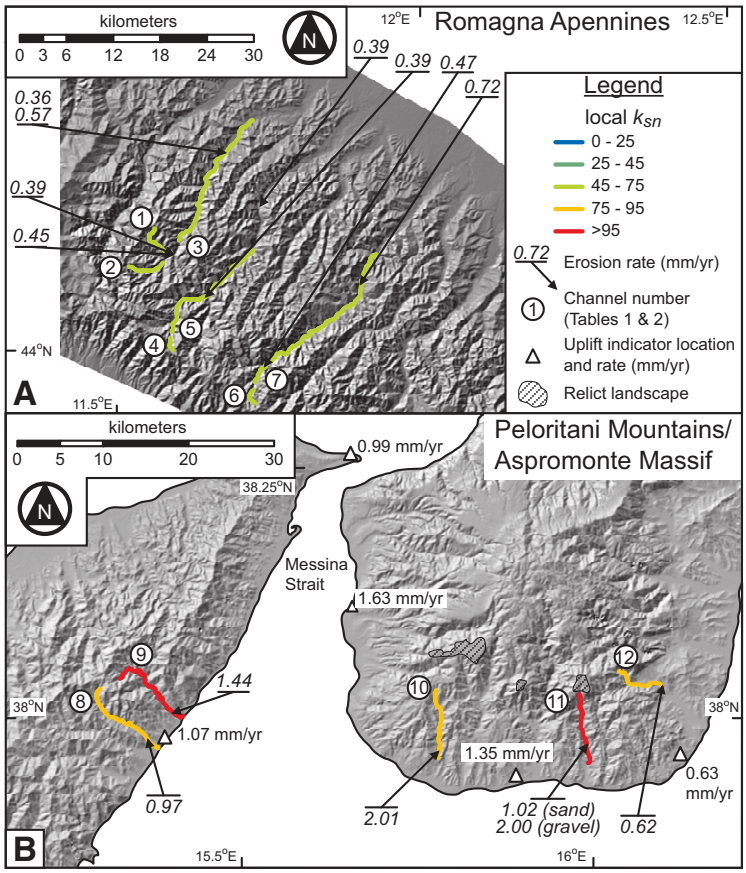

Figure 3. Maps of the Romagna Apennines (A) and Peloritani-Aspromonte (B) study areas showing the distribution of ^{10}Be erosion rates (arrows indicate sample location) and k_{sn} values. White triangles show the locations of marine terraces and associated uplift rates since ca. 125 ka used in our analysis, and hatched areas show the distribution of uplifted relict landscape (refer to text for details).

concentrations of stream sediments from the Romagna Apennines and Peloritani-Aspromonte are presented in Table 2 and Figures 3 and 4. Erosion rates in the Romagna Apennines range from 0.36 ± 0.04 to 0.72 ± 0.14 mm/yr and have a regional mean of 0.46 ± 0.04 (SE) mm/yr. These erosion rates are slightly higher than those reported in Cyr and Granger (2008) because of the muogenic contribution to ^{10}Be concentrations, which was not accounted for in their calculations. Catchment-averaged erosion rates in the Romagna Apennines do not show any pattern with respect to elevation within watersheds or location within the mountain range. Two samples collected from the same location (Table 2, samples 3A and 3B), but at different times of the year, yield erosion rates of 0.36 ± 0.04 mm/yr and 0.57 ± 0.12 mm/yr. This degree of variability is not unexpected with cosmogenic nuclide–based erosion rates, particularly in catchments where hillslope erosion is dominated by mass wasting and where sediments may not be fully mixed (e.g., Granger et al., 1996; Niemi et al., 2005; Yanites et al., 2009). Erosion rates in the Peloritani-Aspromonte are higher than those in the Romagna Apennines and have greater variability, ranging from 0.62 ± 0.06 to 2.01 ± 0.27 mm/yr with a regional mean of 1.21 ± 0.23 (SE) mm/yr. Erosion rates are higher in catchments closest to the Messina Strait, where rock uplift rates are highest (Fig. 3).

DISCUSSION

Both the k_{sn} values of stream channels and ^{10}Be hillslope erosion rates in the Romagna Apennines and Peloritani-Aspromonte increase as a function of increasing rock uplift rates (Fig. 4). The correlation of both k_{sn} values and ^{10}Be erosion rates with rock uplift rates (1) validates our assumption that the Romagna Apennines and Peloritani-Aspromonte landscapes approach steady state, and (2) indicates that both k_{sn} indices and catchment-averaged erosion rates might be useful for quantifying rock uplift rates. However, while both k_{sn} values and catchment-averaged erosion rates increase with increasing rock uplift rates, the nature of these relationships warrants further discussion.

Channel Steepness Values and Rock Uplift Rates

Normalized channel steepness index values in the Romagna Apennines and Peloritani-Aspromonte are compared to long-term rock uplift rates in Figure 4A. In general, k_{sn} values in the Romagna Apennines, which have been uplifting at 0.2–0.5 mm/yr since ca. 0.9 Ma

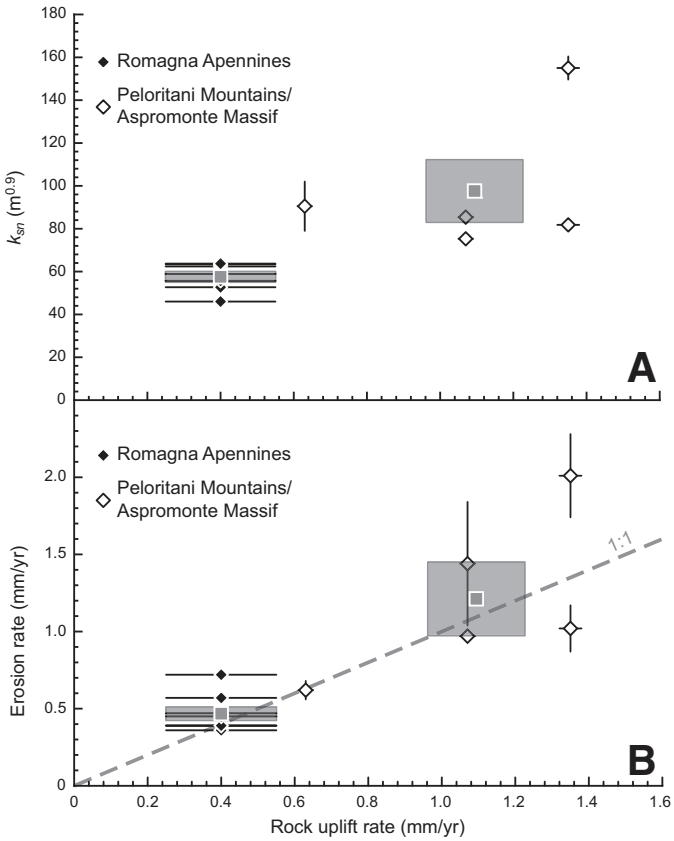

Figure 4. Comparison of k_{sn} values (A) and ^{10}Be erosion rates (B) to rock uplift rates in the Romagna Apennines (filled diamonds) and Peloritani-Aspromonte (open diamonds) study areas. Uncertainties for k_{sn} and erosion rates are 1σ analytical uncertainty. Uncertainties in rock uplift rates are from the literature (see text for references). Gray squares indicate the regional mean k_{sn} values and erosion rates compared to regional mean rock uplift rates and are surrounded by one standard error (calculated as $\sigma/\sqrt{N}$, where σ is one standard deviation of the measurements, and N is the number of measurements used to calculate the mean).

(Picotti and Pazzaglia, 2008; Wegmann and Pazzaglia, 2009), are lower than k_{sn} values in the Peloritani-Aspromonte, where rock uplift rates are between 0.69 and 1.63 mm/yr since at least 125 ka (Cosentino and Gliozzi, 1988; Miayuchi et al., 1994; Bordoni and Valensise, 1998; Ferranti et al., 2006). This relationship is consistent with both theoretical predictions (e.g., Whipple and Tucker, 1999), as well as previous field studies (e.g., Snyder et al., 2000; Kirby and Whipple, 2001; Lague and Davy, 2003; Duvall et al., 2004; Wobus et al., 2006), which all document higher k_{sn} values at increasingly rapid rock uplift rates.

In the Romagna Apennines ($46.0 \pm 1.0 \leq k_{sn} \leq 63.7 \pm 1.5$ m$^{0.9}$), k_{sn} values are generally higher in downstream channel reaches closest to the mountain front. Systematic downstream increases in k_{sn} values could be the result of a variety of factors (e.g., Whipple, 2004), including (1) downstream increases in grain size, bed load, and/or channel width, (2) orographically enhanced precipitation, or (3) higher rock uplift rates, U, in the downstream portions of the analyzed channels. In the case of either downstream increases in sediment caliber or channel width, or of orographically enhanced precipitation at higher catchment elevations, k_{sn} values would decrease downstream, whereas if U increases downstream, k_{sn} values should also increase (e.g., Whipple and Tucker, 1999; Snyder et al., 2000; Kirby and Whipple, 2001; Lague and Davy, 2003; Duvall et al., 2004; Whipple, 2004; Wobus et al., 2006). Although it is likely that the Romagna Apennines approach steady state (Cyr and Granger, 2008), fluvial terrace stratigraphy elsewhere in the northern and central Apennines indicates that rock uplift rates are higher at the mountain front and have accelerated since ca. 140 ka due to active fold growth (Picotti and Pazzaglia, 2008; Wegmann and Pazzaglia, 2009). While variations in bed state or channel width cannot be ruled out as a possible cause for the observed variation in k_{sn} across the Romagna Apennines and Peloritani-Aspromonte, it is more likely that the observed k_{sn} values reflect actively growing structures at the Apennines mountain front (e.g., Picotti and Pazzaglia, 2008; Wegmann and Pazzaglia, 2009). In the Peloritani-Aspromonte region, k_{sn} values increase as a function of rock uplift rate (Figs. 3 and 4; Tables 1 and 2). This is consistent with both the relationship between U and k_{sn} predicted by Equation 3, as well as empirical studies conducted in landscapes where rock uplift rates are known.

It is also possible that the patterns of k_{sn} values observed in both landscapes are the result of the chosen value of θ_{ref}. Normalized channel steepness index values calculated using a range of θ_{ref} between 0.2 and 0.7 are presented in Table DR2 and Figure DR4 (see footnote 1). Although the absolute values of k_{sn} vary over several orders of magnitude depending on the selected value of θ_{ref} (Table DR2 [see footnote 1]), the relationship between k_{sn} and rock uplift rates is maintained (Fig. DR4 [see footnote 1]).

Regardless of the chosen value of θ_{ref}, our data indicate that the k_{sn} values of detachment-limited stream channels in the Romagna Apennines and Peloritani-Aspromonte do increase as a function of increasing rock uplift rates, which is consistent with both theoretical predictions and field observations. It also appears that the relationship between k_{sn} and rock uplift rate is nonlinear, with k_{sn} reaching a threshold at rock uplift rates greater than ~1 mm/yr. The small number of our k_{sn} data points makes a quantitative relationship between k_{sn} and rock uplift rates in the Romagna Apennines and Peloritani and Aspromonte Massif difficult to define. However, if we assume a linear relationship between k_{sn} values and rock uplift rate, the threshold k_{sn} required to initiate channel incision is 43.15 ± 12.20 m$^{0.9}$ (assuming $\theta_{ref} = 0.45$).

Erosion Rates and Rock Uplift Rates

Erosion rate data from both the Romagna Apennines and Peloritani-Aspromonte suggest a correlation with local rock uplift rates as determined from fluvial and marine terrace stratigraphy (Figs. 3 and 4; Table 2). In both of these landscapes, catchment-averaged hillslope erosion rates are similar to local rock uplift rates to within a factor of ~2. This variability might be related to either (1) the stochastic nature of hillslope landsliding and insufficient mixing of landslide-derived sediment in the sampled stream channels (e.g., Granger et al., 1996; Niemi et al., 2005; Yanites et al., 2009), and/or (2) the observed

TABLE 2. COSMOGENIC NUCLIDE DATA, MILLENNIAL-SCALE EROSION RATES, AND ROCK UPLIFT RATES IN THE ROMAGNA APENNINES, PELORITANI MOUNTAINS, AND ASPROMONTE MASSIF

Sample (river at location)	Location* (DD °N/°E)	[^{10}Be]† (10^3 at/g quartz)	Elevation§ (m)	Production rate# (at/g quartz/yr)	Erosion rate** (mm/yr)	Rock uplift rate†† (mm/yr)
Romagna Apennines§§						
1. Visano at Palazzuolo	44.115359/11.541561	16.8 ± 1.8	703	9.18	0.39 ± 0.05	0.40 ± 0.15
2. Senio at Palazzuolo	44.109322/11.537214	14.9 ± 2.4	723	9.34	0.45 ± 0.09	0.40 ± 0.15
3. Senio at Casola (A)	44.221099/11.621287	16.1 ± 1.3	517	7.86	0.36 ± 0.04	0.40 ± 0.15
3. Senio at Casola (B)	44.221099/11.621287	10.2 ± 1.8	517	7.86	0.57 ± 0.12	0.40 ± 0.15
4. Lamone at Biforco	44.064788/11.598059	17.7 ± 0.9	743	9.49	0.39 ± 0.02	0.40 ± 0.15
5. Lamone at San Eufemia	44.169898/11.686457	16.1 ± 0.8	646	8.76	0.39 ± 0.03	0.40 ± 0.15
6. Montone at San Benedetto in Alpi	43.981741/11.688390	15.6 ± 2.4	835	10.24	0.47 ± 0.09	0.40 ± 0.15
7. Montone at Davadola	44.118721/11.884911	8.4 ± 1.3	570	8.22	0.72 ± 0.14	0.40 ± 0.15
Peloritani Mountains						
8. Pagliara at Roccalumera	37.966618/15.38116	5.9 ± 0.4	604	7.82	0.97 ± 0.11	1.07 ± 0.02
9. Fiumedinisi at Nizza di Sicilia	38.00270/15.40523	4.2 ± 1.1	666	8.21	1.44 ± 0.40	1.07 ± 0.02
Aspromonte Massif						
10. San Elia at Pentedáttilo	37.94329/15.75762	2.8 ± 0.3	571	7.61	2.01 ± 0.27	1.35 ± 0.03
11. San Pasquale at Palizzi (sand)	37.94841/15.96210	5.4 ± 0.6	531	7.36	1.02 ± 0.27	1.35 ± 0.03
11. San Pasquale at Palizzi (gravel)	37.94841/15.96210	2.8 ± 0.9	531	7.36	2.00 ± 0.65	1.35 ± 0.03
12. Torno at Bruzzano Zeffírio	38.00476/16.08362	7.9 ± 0.5	397	6.61	0.62 ± 0.06	0.69 ± 0.02

*WGS84 datum.
†[^{10}Be] measured by accelerator mass spectrometry at Prime Laboratory, Purdue University, against standards prepared by K. Nishiizumi. Concentrations have been decreased by 14% to correct for a ^{10}Be half-life of 1.34 m.y. (Nishiizumi et al., 2007).
§Elevation is the area-weighted catchment-averaged elevation of the catchment above the sample location.
#Production rate is the spatially averaged production rate over the catchment, scaled for elevation and latitude according to Stone (2000), using a sea-level, high-latitude production rate of 5.1 at/g/yr decreased by 14% based on a ^{10}Be half-life of 1.34 m.y. (Nishiizumi et al., 2007).
**Quoted uncertainty is the analytical uncertainty only and does not include an ~7% uncertainty in the sea-level, high-latitude ^{10}Be production rate.
††Refer to text for uplift rate sources.
§§Location is the name of the town nearest to where the sample was collected, according to the Millennial edition of *Atlante Stradale d'Italia* by the Touring Club Italiano.

spatial pattern of Quaternary rock uplift rates. This variability makes it unlikely that any one erosion rate from a single drainage basin will accurately quantify millennial-scale rock uplift rates. However, in catchments where hillslope erosion is dominated by shallow landsliding, determinations of erosion rates from ^{10}Be concentrations of sediment samples collected from multiple non-nested catchments should converge on the long-term average concentration of ^{10}Be and reflect true millennial-scale catchment-averaged erosion rates (Niemi et al., 2005; Yanites et al., 2009).

In this case, the data can be considered as two groups of catchments representing landscapes where rock uplift rates are relatively slow (the Romagna) and relatively rapid (the Peloritani-Aspromonte). If the data are treated in this way, the regional mean hillslope erosion rates are indistinguishable from the regional mean rock uplift rates within one standard error of the mean (Fig. 4). This result is perhaps not surprising, given the predictions of various conceptual and numerical landscape evolution models that have described a similar functional relationship between hillslope erosion rates and rock uplift rates, and it demonstrates the potential for ^{10}Be-determined, catchment-averaged hillslope erosion rates to be used as a proxy for millennial-scale rock uplift rates.

Steady-State Assumption in the Romagna Apennines and Peloritani-Aspromonte

Our use of k_{sn} values and ^{10}Be catchment-averaged erosion rates to quantify absolute rock uplift rates depends on the underlying assumption that the Romagna Apennines and Peloritani-Aspromonte landscapes approach steady state. Some studies have demonstrated that a variety of landscapes around the world may approach steady-state conditions by demonstrating that erosion rates are similar to long-term exhumation rates (e.g., Matmon et al., 2003; Vance et al., 2003; Safran et al., 2005), or that one or both k_{sn} values and ^{10}Be erosion rates are sensitive to spatially variable tectonic forcing (e.g., Wobus et al., 2005, 2006). However, it has also been suggested that steady-state conditions may never be reached, since the adjustment time scales of hillslope and channel systems may be longer than either the climatic (e.g., Zhang et al., 2001) or tectonic fluctuations to which they respond.

Despite the argument that steady state may be difficult to achieve and/or maintain over geologic time scales (>10^4 yr), there is evidence that some of our field areas do approach steady state. In a comparison of ^{10}Be erosion and paleoerosion rates to long- and short-term erosion, channel incision, and rock uplift rates, Cyr and Granger (2008) demonstrated that the Romagna Apennines approach steady state. In this case, erosion and paleoerosion rates were similar to (1) short-term (decadal) sediment yield determined from reservoir sedimentation, (2) long-term (10^6 yr) sediment yield determined from basin sedimentation, (3) fluvial incision rates determined from terrace stratigraphy (over 10^5 yr), (4) mountain uplift rates from geodetic re-leveling (over 10^2 yr), (5) coastal uplift rates from uplifted shorelines (over 10^5 yr), and (6) long-term (10^6 yr) exhumation rates from thermochronometry, indicating steady-state conditions in the Romagna Apennines since at least 0.9 Ma.

There are no similar data indicating that the Peloritani-Aspromonte approach steady state, besides making the qualitative argument that the channel morphology exhibits no clear sign of disequilibrium over the examined portions of channel longitudinal profiles. Regardless, the fact that both k_{sn} values and catchment-averaged erosion vary in proportion to rock uplift rates in the Peloritani-Aspromonte, as well as in the Romagna Apennines, both tests and confirms our initial steady-state assumption. This sort of integrated approach, combining both k_{sn} analysis and ^{10}Be erosion rate determinations, may be useful for identifying possible steady-state conditions in landscapes where the degree of steady state is unknown.

Comparing Channel Steepness and Erosion Rates

Individually, both calculated k_{sn} values and ^{10}Be-determined hillslope erosion rates have limitations as tools for describing absolute rock uplift rates. Determinations of the k_{sn} values of channels draining the Romagna Apennines and Peloritani-Aspromonte, while broadly indicative of relative differences in rock uplift rates across a given area, do not appear to increase indefinitely with increasing rock uplift rates. This potentially limits the utility of k_{sn} for quantifying spatial variations in rock uplift rates in rapidly uplifting landscapes. Catchment-averaged hillslope erosion rates, on the other hand, are locally similar to long-term (10^5 yr) rock uplift rates in both relatively slowly and relatively rapidly uplifting landscapes. Erosion rates appear to increase roughly linearly with rock uplift rates in all cases. However, based on repeat erosion rate determinations at one sampling location (Table 2), any single erosion rate measurement is different from the local rock uplift rate by up to a factor of ~2, making it unlikely that any single determination of an erosion rate in an individual catchment can be used to reliably quantify rock uplift rate. The combination of detachment-limited channel profile analysis and determinations of catchment-averaged hillslope erosion rates using ^{10}Be might be a more effective way to (1) establish that a landscape approaches steady state with tectonically driven rock uplift; (2) identify landscapes where rock uplift rates might be similar; and (3) quantify rock uplift rates by using the erosion rates of several catchments across a region and averaging those rates together.

Lithologically uniform drainage basins that approach steady state should exhibit uniform k_{sn} values and catchment-averaged erosion rates. Catchments where all segments of the drainage network have similar k_{sn} values suggest spatially uniform K and U (Eq. 1). In these cases, channel incision rates should scale with rock uplift rates, and an average of ^{10}Be erosion rates in these catchments should equal the regional average rock uplift rate. The distributions of k_{sn} values and catchment-averaged hillslope erosion rates might also be useful for distinguishing landscapes with different tectonic forcing. In addition to determining whether channel incision rates approach steady state with rock uplift rates, channel steepness analyses could be used to identify where changes in tectonic forcing might occur. Catchments with internally similar k_{sn} values in one landscape that are different from those in another landscape, such as those between the Romagna Apennines and Peloritani-Aspromonte, suggest that the two drainage networks have equilibrated to different sets of K and/or U values. Assuming steady-state conditions, the spatial pattern of k_{sn} values could be used to inform cosmogenic nuclide sampling strategies with the goal of using the average erosion rates of several catchments across a region to quantify regional average rock uplift rates.

CONCLUSIONS

The Romagna Apennines, northern Italy, and the Peloritani Mountains and Aspromonte Massif, southern Italy, are landscapes that have broadly similar climate and lithologic resistance to erosion, but that record markedly different rock uplift rates over at least the past 125 k.y., as indicated by fluvial and marine terrace stratigraphy. We calculated normalized channel steepness index (k_{sn}) values and cosmogenic ^{10}Be erosion rates in eight catchments where rock uplift rates inferred from fluvial and marine terrace stratigraphy increase from 0.40 ± 0.15 mm/yr to 1.35 ± 0.03 mm/yr. We find that:

(1) k_{sn} values increase with rock uplift rates up to ~1 mm/yr, above which they appear to reach a threshold value; and

(2) ^{10}Be erosion rates increase linearly with increasing rock uplift rates. Based on repeat measurements, individual determinations of erosion rate are only similar to local rock uplift rates to within a factor of ~2. However, regional average erosion rates in each of our landscapes are indistinguishable from the regional mean rock uplift rates.

Collectively, our k_{sn} and erosion rate data indicate that these methods can be combined as a tool to quantify rock uplift rates. Channel steepness index calculations could be used to inform field mapping in order to assess the effects of changes in channel width, bed cover, rock resistance to erosion, etc., and sediment sampling for the determination of erosion rates using cosmogenic nuclides. This would allow the determination of regionally (≥100 km^2) averaged rock uplift rates using catchment-averaged erosion rates by maximizing the effects of tectonically driven rock uplift rates on the sampled catchments, while simultaneously minimizing the complications inherent in both methods.

ACKNOWLEDGMENTS

This project was supported by National Science Foundation Continental Dynamics Program grant EAR-0208169 (RETREAT), PRIME Laboratory at Purdue University, and the U.S. Geological Survey Mendenhall Postdoctoral Fellowship program. This manuscript benefited from comments by Thomas Hanks, Stephen DeLong, reviews by Brian Yanites and an anonymous reviewer, and editorial guidance from Jon Pelletier.

REFERENCES CITED

Amodio Morelli, L., Bonardi, G., Colonna, V., Dietrich, D., Giunta, G., Ippolito, F., Liguori, V., Lorenzoni, S., Paglianico, A., Perrone, V., Piccarreta, G., Russo, M., Scandone, P., Zanettin Lorenzoni, E., and Zuppetta, A., 1976, L'Arco Calabro-Peloritano nell'orogene Appenninico-Maghrebide: Bolletino della Societa Geologica Italiana, v. 17, p. 1–60.

Bartolini, C., 2003, When did the Northern Apennines become a mountain chain?: Quaternary International, v. 101–102, p. 75–80, doi: 10.1016/S1040-6182(02)00090-3.

Bierman, P.R., and Steig, E.J., 1996, Estimating rates of denudation using cosmogenic isotope abundances in sediment: Earth Surface Processes and Landforms, v. 21, p. 125–139, doi: 10.1002/(SICI)1096-9837(199602)21:2<125::AID-ESP511>3.0.CO;2-8.

Bonardi, G., Giunta, G., Perrone, B., Russo, M., Zuppetta, A., and Ciampo, G., 1980, Osservazioni sull'evoluzione dell'Arco Calabro Peloritano nel Miocene inferiore: La Formazione di Stilo Capo d'Orlando: Bolletino della Societa Geologica Italiana, v. 99, p. 365–393.

Bordoni, P., and Valensise, G., 1998, Deformation of the 125-ka marine terrace in Italy: Tectonic implications, *in* Stewart, I.S., and Vita-Finzi, C., eds., Coastal Tectonics: Geological Society, London, Special Publication 146, p. 71–110, doi: 10.1144/GSL.SP.1999.146.01.05.

Brown, E.T., Stallard, R.F., Larsen, M.C., Raisbeck, G.M., and Yiou, F., 1995, Denudation rates determined from the accumulation of in situ–produced ^{10}Be in the Luquillo Experimental Forest, Puerto Rico: Earth and Planetary Science Letters, v. 129, p. 193–202, doi: 10.1016/0012-821X(94)00249-X.

Castellarin, A., Eva, C., Giglia, G., and Vai, G.B., 1985, Analisi strutturale del fronte Appenninico Padano: Giornale di Geologia, v. 47, p. 47–76.

Catalano, R., and D'Argenio, B., 1978, An essay of palinspastic restoration across the western Sicily: Geolgica Romana, v. 17, p. 145–159.

Champagnac, J.-D., Schlunegger, F., Norton, K., von Blanckenburg, F., Abbühl, L.M., and Schwab, M., 2009, Erosion-driven uplift of the modern central Alps: Tectonophysics, v. 474, p. 236–249, doi: 10.1016/j.tecto.2009.02.024.

Colalongo, M.L., Nanni, T., and Ricci Lucchi, F., 1979, Sedimentazione ciclica nel Pleistocene Anconetano: Geologica Romana, v. 18, p. 71–92.

Cosentino, D., and Gliozzi, E., 1988, Considerazioni sulle velocitá di sollevamento di depositi Eutirreniani dell'italia Meridionale e della Sicilia: Memorie della Societa Geologica Italiana, v. 41, p. 653–665.

Cyr, A.J., and Granger, D.E., 2008, Dynamic equilibrium among erosion, river incision, and coastal uplift in the northern and central Apennines, Italy: Geology, v. 36, p. 103–106, doi: 10.1130/G24003A.1.

D'Anastasio, E., De Martini, P.M., Selvaggi, G., Pantosti, D., Marchioni, A., and Maseroli, R., 2006, Short-term vertical velocity field in the Apennines (Italy) revealed by geodetic levelling data: Tectonophysics, v. 418, p. 219–234, doi: 10.1016/j.tecto.2006.02.008.

Del Maschio, L., Gozza, G., Pignone, S., and Pizziolo, M., 2005, Determinazione di soglie pluviometriche per innesco di fenomeni franosi nell'Apennino settentrionale: 1st Report on Convenzione Tra Arpa-Servizio Idrologico Regionale e Servizio Geologico Sismico e dei Suoli Regional per il Supporto alle Attività del Centro Funzionale, Regione Emilia-Romagna: http://www.regione.emilia-romagna.it/wcm/geologia/canali/frane/rel_scien/val_risch_fr/soglie_pluviometriche.pdf (accessed August 2007).

Dietrich, W.E., Wilson, C.J., Montgomery, D.R., and McKean, J., 1993, Analysis of erosion thresholds, channel networks, and landscape morphology using a digital terrain model: The Journal of Geology, v. 101, p. 259–278, doi: 10.1086/648220.

Duvall, A., Kirby, E., and Burbank, D.W., 2004, Tectonic and lithologic controls on bedrock channel profiles and processes in coastal California: Journal of

Geophysical Research–Earth Surface, v. 109, F03002, doi: 10.1029/2003JF000086.

Faccenna, C., Funicello, F., Giardini, D., and Lucente, P., 2001, Episodic back-arc extension during restricted mantle convection in the Central Mediterranean: Earth and Planetary Science Letters, v. 187, p. 105–116, doi: 10.1016/S0012-821X(01)00280-1.

Faccenna, C., Piromallo, C., Crespo-Blanc, A., Jolivet, L., and Rossetti, F., 2004, Lateral slab deformation and the origin of the Western Mediterranean arcs: Tectonics, v. 23, TC1012, doi: 10.1029/2002TC001488.

Falguères, C., 2003, ESR dating and the human evolution: Contribution to the chronology of the earliest humans in Europe: Quaternary Science Reviews, v. 22, p. 1345–1351, doi: 10.1016/S0277-3791(03)00047-7.

Feroni, A.C., Leoni, L., Martelli, L., Martinelli, P., Ottria, G., and Sarti, G., 2001, The Romagna Apennines, Italy: An eroded duplex: Geological Journal, v. 36, p. 39–45, doi: 10.1002/gj.874.

Ferranti, L., Antonioli, A., Mauz, B., Amorosi, A., Dai Pra, G., Mastronuzzi, G., Monaco, C., Orru, P., Pappalardo, M., Radtke, U., Renda, P., Romano, P., Sanso, P., and Verrubbi, V., 2006, Markers of the last interglacial highstand along the coast of Italy: Tectonic implications: Quaternary International, v. 145–146, p. 30–54, doi: 10.1016/j.quaint.2005.07.009.

Ferrier, K.L., Kirchner, J.W., and Finkel, R.C., 2005, Erosion rates over millennial and decadal timescales at Caspar Creek and Redwood Creek, northern California Coast Ranges: Earth Surface Processes and Landforms, v. 30, p. 1025–1038, doi: 10.1002/esp.1260.

Flint, J.J., 1974, Stream gradient as a function of order, magnitude, and discharge: Water Resources Research, v. 10, p. 969–973, doi: 10.1029/WR010i005p00969.

Gagnepain, J., Hedley, I., Bahain, J.J., Falguères, C., Laurent, M., Peretto, C., Wagner, J.J., and Yokoyama, Y., 1996, Synthèse des données radiochronologique et paléomagnétiques du site de Ca'Belvedere di Monte Poggiolo (Romagna, Italie) et de son environnement géologique, *in* Proceedings, XIIIe Congrès Union Internationale des Sciences Prééhistoriques et Protohistoriques: Forlí, Italy, The Workshops, A.B.A.C.O., abs. 2, p. 129–130.

Granger, D.E., and Smith, A.L., 2000, Dating buried sediments using radioactive decay and muogenic production of ^{26}Al and ^{10}Be: Nuclear Instruments & Methods in Physics Research, Section B, Beam Interactions with Materials and Atoms, v. 172, p. 822–826, doi: 10.1016/S0168-583X(00)00087-2.

Granger, D.E., Kirchner, J.W., and Finkel, R., 1996, Spatially averaged long-term erosion rates measured from in situ–produced cosmogenic nuclides in alluvial sediment: The Journal of Geology, v. 104, p. 249–257, doi: 10.1086/629823.

Granger, D.E., Riebe, C.S., Kirchner, J.W., and Finkel, R., 2001, Modulation of erosion on steep granitic slopes by boulder armoring, as revealed by cosmogenic ^{26}Al and ^{10}Be: Earth and Planetary Science Letters, v. 186, p. 269–281, doi: 10.1016/S0012-821X(01)00236-9.

Gurrola, L.D., Keller, E.A., Trecker, M.A., Hartleb, R.D., and Dibblee, T.W., 1998, Active folding and reverse faulting, Santa Barbara fold belt, California, *in* Behl, R., ed., Geological Society of America Fieldtrip Guidebook, 94th Annual Meeting, Cordilleran Section: Boulder, Colorado, Geological Society of America, p. 1–43.

Hack, J.T., 1957, Studies of Longitudinal Stream Profiles in Virginia and Maryland: U.S. Geological Survey Professional Paper 294-B, 97 p.

Hack, J.T., 1960, Interpretation of erosional topography in humid temperate regions: American Journal of Science, v. 258-A, p. 80–97.

Hancock, G.S., Anderson, R.S., and Whipple, K.X., 1998, Beyond power: Bedrock river incision process and form, *in*, Tinkler, K.J., and Wohl, E.E., eds., Rivers Over Rock: Fluvial Processes in Bedrock Channels: American Geophysical Union Geophysical Monograph 107, p. 35–60.

Hancock, G.S., Anderson, R.S., Chadwick, O.A., and Finkel, R.C., 1999, Dating fluvial terraces with ^{10}Be and ^{26}Al profiles: Application to the Wind River, Wyoming: Geomorphology, v. 27, p. 41–60, doi: 10.1016/S0169-555X(98)00089-0.

Hippolyte, J.C., Angelier, J., and Roure, F., 1994, A major geodynamic change revealed by Quaternary stress patterns in the Southern Apennines, Italy: Tectonophysics, v. 230, p. 199–210, doi: 10.1016/0040-1951(94)90135-X.

Howard, A.D., and Kerby, G., 1983, Channel changes in badlands: Geological Society of America Bulletin, v. 94, p. 739–752, doi: 10.1130/0016-7606(1983)94<739:CCIB>2.0.CO;2.

Howard, A.D., Seidl, M.A., and Dietrich, W.E., 1994, Modeling fluvial erosion on regional to continental scales: Journal of Geophysical Research, v. 99, p. 13,971–13,986, doi: 10.1029/94JB00744.

Ietto, F., Ferdinando Donato, F., and Ietto, A., 2007, Recent reverse faults and landslides in granitoid weathered profiles, Serre Mountains (southern Calabria, Italy): Geomorphology, v. 87, p. 196–206, doi: 10.1016/j.geomorph.2006.03.042.

Kirby, E., and Whipple, K.X., 2001, Quantifying differential rock-uplift rates via stream profile analysis: Geology, v. 29, p. 415–418, doi: 10.1130/0091-7613(2001)029<0415:QDRURV>2.0.CO;2.

Kirby, E., Whipple, K.X., Tang, W., Chen, Z., 2003, Distribution of active rock uplift along the eastern margin of the Tibetan Plateau: Inferences from bedrock river profiles: Journal of Geophysical Research, v. 108, no. B4, 2217, doi: 10.1029/2001JB000861.

Kirby, E., Johnson, C., Furlong, K., and Heimsath, A.M., 2007, Transient channel incision along Bolinas Ridge, California: Evidence for differential rock uplift adjacent to the San Andreas fault: Journal of Geophysical Research–Earth Surface, v. 112, F03S07, doi: 10.1029/2006JF000559.

Kirchner, J.W., Finkel, R., Riebe, C.S., Granger, D.E., Clayton, J.L., King, J.G., and Megahan, W.F., 2001, Mountain erosion over 10 yr, 10 k.y., and 10 m.y. time scales: Geology, v. 29, p. 591–594, doi: 10.1130/0091-7613(2001)029<0591:MEOYKY>2.0.CO;2.

Kobor, J.S., and Roering, J.J., 2004, Systematic variation of bedrock channel gradients in the central Oregon Coast Range: Implications for rock uplift and shallow landsliding: Geomorphology, v. 62, p. 239–256, doi: 10.1016/j.geomorph.2004.02.013.

Lague, D., and Davy, P., 2003, Constraints on the long-term colluvial erosion law by analyzing slope-area relationships at various tectonic uplift rates in the Siwalik Hills (Nepal): Journal of Geophysical Research–Solid Earth, v. 108, doi: 10.1029/2002JB001893.

Lague, D., Davy, P., and Crave, A., 2000, Estimating uplift rate and erodibility from the area-slope relationship: Examples from Brittany (France) and numerical modelling: Physics and Chemistry of the Earth, v. 25, p. 543–548, doi: 10.1016/S1464-1895(00)00083-1.

Lavé, J., and Avouac, J.P., 2001, Fluvial incision and tectonic uplift across the Himalayas of central Nepal: Journal of Geophysical Research–Solid Earth, v. 106, p. 26,561–26,591, doi: 10.1029/2001JB000359.

Le Pera, E., and Sorriso-Valvo, M., 2000, Weathering and morphogenesis in a Mediterranean climate, Calabria, Italy: Geomorphology, v. 34, p. 251–270, doi: 10.1016/S0169-555X(00)00012-X.

Marabini, S., Taviani, M., Vai, G.B., and Vigliotti, L., 1995, Yellow sand facies with *Arctica islandica*: Low-stand signature in an early Pleistocene front-Apennine basin: Giornale di Geologia, v. 57, p. 259–275.

Masarik, J., and Reedy, R.C., 1995, Terrestrial cosmogenic-nuclide production systematics calculated from numerical simulations: Earth and Planetary Science Letters, v. 136, p. 381–395, doi: 10.1016/0012-821X(95)00169-D.

Matmon, A., Bierman, P.R., Larsen, J., Southworth, S., Pavich, M.J., and Caffee, M.W., 2003, Temporally and spatially uniform rates of erosion in the southern Appalachian Great Smoky Mountains: Geology, v. 31, p. 155–158, doi: 10.1130/0091-7613(2003)031<0155:TASURO>2.0.CO;2.

Merritts, D., and Bull, W.B., 1989, Interpreting Quaternary uplift rates at Mendocino triple junction, northern California, from uplifted marine terraces: Geology, v. 17, p. 1020–1024, doi: 10.1130/0091-7613(1989)017<1020:IQURAT>2.3.CO;2.

Merritts, D.J., Vincent, K.R., and Wohl, E.E., 1994, Long river profiles, tectonism, and eustasy: A guide to interpreting fluvial terraces: Journal of Geophysical Research–Solid Earth, v. 99, p. 14,031–14,050, doi: 10.1029/94JB00857.

Metcalf, J.G., 1994, Morphology, Chronology, and Deformation of Pleistocene Marine Terraces, Southwestern Santa Barbara County, California [M.S. thesis]: Santa Barbara, University of California, 167 p.

Miayuchi, T., Dai Pra, G., and Sylos Labini, S., 1994, Geochronology of Pleistocene marine terraces and regional tectonics in the Tyrrhenian coast of south Calabria, Italy: Il Quarternario, v. 7, p. 17–33.

Molnar, P., and England, P., 1990, Late Cenozoic uplift of mountain ranges and global climate change: Chicken or egg?: Nature, v. 346, p. 29–34, doi: 10.1038/346029a0.

Montgomery, D.R., and Foufoula-Georgiou, E., 1993, Channel network source representation using digital elevation models: Water Resources Research, v. 29, p. 3925–3934, doi: 10.1029/93WR02463.

Niemi, N.A., Oskin, M., Burbank, D.W., Heimsath, A., and Gabet, E.J., 2005, Effects of bedrock landslides on cosmogenically determined erosion rates: Earth and Planetary Science Letters, v. 237, p. 480–498, doi: 10.1016/j.epsl.2005.07.009.

Nigro, F., 1996, Late Oligocene–early Miocene sedimentary evolution of the foreland basins in the Sicilian mobile belt: The example of the Peloritani area: Terra Nova, v. 8, p. 611–625, doi: 10.1111/j.1365-3121.1996.tb00791.x.

Nishiizumi, K., Imamura, M., Caffee, M.W., Southon, J.R., Finkel, R.C., McAninch, J., 2007, Absolute calibration of ^{10}Be AMS standards: Nuclear Instruments and Methods in Physics Research B, v. 258, p. 403–413, doi: 10.1016/j.nimb.2007.01.297.

Ouimet, W.B., Whipple, K.X., and Granger, D.E., 2009, Beyond threshold hillslopes: Channel adjustment to base-level fall in tectonically active mountain ranges: Geology, v. 37, p. 579–582, doi: 10.1130/G30013A.1.

Pan, B.T., Burbank, D., Wang, Y.X., Wu, G.J., Li, J.J., and Guan, Q.Y., 2003, A 900 k.y. record of strath terrace formation during glacial-interglacial transitions in northwest China: Geology, v. 31, p. 957–960, doi: 10.1130/G19685.1.

Pazzaglia, F.J., and Gardner, T.W., 1993, Fluvial terraces of the lower Susquehanna River: Geomorphology, v. 8, p. 83–113, doi: 10.1016/0169-555X(93)90031-V.

Pellegrino, A., and Prestininzi, A., 2007, Impact of weathering on the geomechanical properties of rocks along thermal-metamorphic contact belts and morpho-evolutionary processes: The deep-seated gravitational slope deformations of Mt. Granieri-Salincriti (Calabria-Italy): Geomorphology, v. 87, p. 176–195, doi: 10.1016/j.geomorph.2006.03.032.

Picotti, V., and Pazzaglia, F.J., 2008, A new active tectonic model for the construction of the Northern Apennines mountain front near Bologna (Italy): Journal of Geophysical Research–Solid Earth, v. 113, B08412, doi: 10.1029/2007JB005307.

Platt, J.P., and Compagnoni, R., 1990, Alpine ductile deformation and metamorphism in a Calabrian basement nappe (Aspromonte, south Italy): Eclogae Geologicae Helvetiae, v. 83, p. 41–58.

Ricci Lucchi, F., 1986, The Oligocene to Recent foreland basins of the northern Apennines, *in* Allen, P.A., and Homewood, P., eds., Foreland Basins: International Association of Sedimentologists Special Publication 8, p. 105–139.

Riebe, C.S., Kirchner, J.W., Granger, D.E., and Finkel, R., 2001, Minimal climatic control on erosion rates in the Sierra Nevada, California: Geology, v. 29, p. 447–450, doi: 10.1130/0091-7613(2001)029<0447:MCCOER>2.0.CO;2.

Safran, E.B., Bierman, P.R., Aalto, R., Dunne, T., Whipple, K.X., and Caffee, M.W., 2005, Erosion rates driven by channel network incision in the Bolivian Andes: Earth Surface Processes and Landforms, v. 30, p. 1007–1024, doi: 10.1002/esp.1259.

Schaller, M., and Ehlers, T.A., 2006, Limits to quantifying climate driven changes in denudation rates with cosmogenic radionuclides: Earth and Planetary Science Letters, v. 248, p. 153–167, doi: 10.1016/j.epsl.2006.05.027.

Schumm, S.A., and Lichty, R.W., 1965, Time, space, and causality in geomorphology: American Journal of Science, v. 263, p. 110–119.

Simoni, A., Elmi, C., and Picotti, V., 2003, Late Quaternary uplift and valley incision in the Northern Apennines: Lamone catchment: Quaternary International, v. 101–102, p. 253–267, doi: 10.1016/S1040-6182(02)00106-4.

Sklar, L., and Dietrich, W.E., 1998, River longitudinal profiles and bedrock incision models: Stream power and the influence of sediment supply, *in* Tinkler, K., and Wohl,

E.E., eds., Rivers Over Rock: Fluvial Processes in Bedrock Channels: American Geophysical Union Geophysical Monograph 107, p. 237–260.

Snyder, N.P., Whipple, K.X., Tucker, G.E., and Merritts, D.J., 2000, Landscape response to tectonic forcing: Digital elevation model analysis of stream profiles in the Mendocino triple junction region, northern California: Geological Society of America Bulletin, v. 112, p. 1250–1263, doi: 10.1130/0016-7606(2000)112<1250:LRTTFD>2.0.CO;2.

Snyder, N.P., Whipple, K.X., and Tucker, G.E., 2003, Importance of a stochastic distribution of floods and erosion thresholds in the bedrock river incision problem: Journal of Geophysical Research–Solid Earth, v. 108, doi: 10.1029/2001JB001655.

Spagnolo, M., and Pazzaglia, F.J., 2005, Testing the geological influences on the evolution of river profiles: A case from the Northern Apennines (Italy): Geografia Fisica e Dinamica Quaternaria, v. 28, p. 103–113.

Stock, G.M., Frankel, K.L., Ehlers, T.A., Schaller, M., Briggs, S.M., and Finkel, R.C., 2009, Spatial and temporal variations in denudation of the Wasatch Mountains, Utah, USA: Lithosphere, v. 1, p. 34–40, doi: 10.1130/L15.1.

Stock, J.D., and Dietrich, W.E., 1998, Channel incision by debris flows: A missing erosion law?: Eos (Transactions, American Geophysical Union), v. 79, no. 45, p. F366.

Stock, J.D., and Dietrich, W.E., 2003, Valley incision by debris flows: Evidence of a topographic signature: Water Resources Research, v. 39, 1089, doi: 10.1029/2001WR001057.

Stock, J.D., and Montgomery, D.R., 1999, Geologic constraints on bedrock river incision using the stream power law: Journal of Geophysical Research–Solid Earth, v. 104, p. 4983–4993, doi: 10.1029/98JB02139.

Stone, J.O., 2000, Air pressure and cosmogenic isotope production: Journal of Geophysical Research, v. 105, p. 23,753–23,759, doi: 10.1029/2000JB900181.

Tarboton, D.G., Bras, R.L., and Rodriguez-Iturbe, I., 1989, Scaling and elevation in river networks: Water Resources Research, v. 25, p. 2037–2051, doi: 10.1029/WR025i009p02037.

Tarboton, D.G., Bras, R.L., and Rodriguez-Iturbe, I., 1991, On the extraction of channel networks from digital elevation data: Hydrological Processes, v. 5, p. 81–100, doi: 10.1002/hyp.3360050107.

Thomson, S.A., 1994, Fission track analysis of the crystalline basement rocks of the Calabrian Arc, southern Italy: Evidence of Oligo-Miocene late-orogenic extension and erosion: Tectonophysics, v. 238, p. 331–352, doi: 10.1016/0040-1951(94)90063-9.

Thomson, S.A., 1998, Assessing the nature of tectonic contacts using fission-track thermochronology: An example from the Calabrian Arc, southern Italy: Terra Nova, v. 10, p. 32–36, doi: 10.1046/j.1365-3121.1998.00165.x.

Trecker, M.A., Gurrola, L.D., and Keller, E.A., 1998, Oxygen-isotope correlation of marine terraces and uplift of the Mesa Hills, Santa Barbara, California, USA, *in* Stewart, I.S., and Vita-Finzi, C., eds., Coastal Tectonics: Geological Society, London, Special Publication 146, p. 57–69, doi: 10.1144/GSL.SP.1999.146.01.04.

Vance, D., Bickle, M., Ivy-Ochs, S., and Kubik, P.W., 2003, Erosion and exhumation in the Himalaya from cosmogenic isotope inventories of river sediments: Earth and Planetary Science Letters, v. 206, p. 273–288, doi: 10.1016/S0012-821X(02)01102-0.

von Blanckenburg, F., 2005, The control mechanisms of erosion and weathering at basin scale from cosmogenic nuclides in river sediment: Earth and Planetary Science Letters, v. 237, p. 462–479, doi: 10.1016/j.epsl.2005.06.030.

Wegmann, K.W., and Pazzaglia, F.J., 2002, Holocene strath terraces, climate change, and active tectonics: The Clearwater River basin, Olympic Peninsula, Washington State: Geological Society of America Bulletin, v. 114, p. 731–744, doi: 10.1130/0016-7606(2002)114<0731:HSTCCA>2.0.CO;2.

Wegmann, K.W., and Pazzaglia, F.J., 2009, Late Quaternary fluvial terraces of the Romagna and Marche Apennines, Italy: Climatic, lithologic, and tectonic controls on terrace genesis in an active orogen: Quaternary Science Reviews, v. 28, p. 137–165, doi: 10.1016/j.quascirev.2008.10.006.

Whipple, K.X., 2004, Bedrock rivers and the geomorphology of active orogens: Annual Review of Earth and Planetary Sciences, v. 32, p. 151–185, doi: 10.1146/annurev.earth.32.101802.120356.

Whipple, K.X., and Tucker, G.E., 1999, Dynamics of the stream-power river incision model: Implications for eight limits of mountain ranges, landscape response timescales, and research needs: Journal of Geophysical Research, v. 104, p. 17,661–17,674, doi: 10.1029/1999JB900120.

Whipple, K.X., Kirby, E., and Brocklehurst, S.H., 1999, Geomorphic limits to climate-induced increases in topographic relief: Nature, v. 401, p. 39–43, doi: 10.1038/43375.

Whipple, K.X., Hancock, G.S., and Anderson, R.S., 2000a, River incision into bedrock: Mechanics and relative efficacy of plucking, abrasion, and cavitation: Geological Society of America Bulletin, v. 112, p. 490–503, doi: 10.1130/0016-7606(2000)112<490:RIIBMA>2.0.CO;2.

Whipple, K.X., Snyder, N.P., and Dollenmayer, K., 2000b, Rates and processes of bedrock incision by the Upper Ukak River since the 1912 Novarupta ash flow in the Valley of Ten Thousand Smokes, Alaska: Geology, v. 28, p. 835–838, doi: 10.1130/0091-7613(2000)28<835:RAPOBI>2.0.CO;2.

Whipple, K.X., Wobus, C., Crosby, B., Kirby, E., and Sheehan, D., 2007, New tools for quantitative geomorphology: Extraction and interpretation of stream profiles from digital topographic data: Geological Society of America Annual Meeting Short Course, 28 October 2007: http://www.geomorphtools.org/Tools/StPro/StPro.htm (accessed August 2008).

Wilson, L.F., Pazzaglia, F.J., and Anastasio, D.J., 2009, A fluvial record of active fault-propagation folding, Salsomaggiore anticline, Northern Apennines, Italy: Journal of Geophysical Research, v. 114, B08403, doi: 10.1029/2008JB005984.

Wittmann, H., von Blanckenburg, F., Kruesmann, T., Norton, K.P., and Kubik, P.W., 2007, Relation between rock uplift and denudation from cosmogenic nuclides in river sediment in the Central Alps of Switzerland: Journal of Geophysical Research, v. 112, F04010, doi: 10.1029/2006JF000729.

Wobus, C., Heimsath, A., Whipple, K.X., and Hodges, K.V., 2005, Active out-of-sequence thrusting in the central Nepalese Himalaya: Nature, v. 434, p. 1008–1011, doi: 10.1038/nature03499.

Wobus, C., Whipple, K.X., Kirby, E., Snyder, N.P., Johnson, J., Spyropolou, K., Crosby, B.T., and Sheehan, D., 2006, Tectonics from topography: Procedures, promise, and pitfalls, *in*, Willett, S.D., Hovius, N., Brandon, M.T., and Fisher, D.M., eds., Tectonics, Climate, and Landscape Evolution: Geological Society of America Special Paper 398, p. 55–74, doi: 10.1130/2006.2398(04).

Yanites, B.J., Tucker, G.E., and Anderson, R.S., 2009, Numerical and analytical models of cosmogenic radionuclide dynamics in landslide-dominated drainage basins: Journal of Geophysical Research–Earth Surface, v. 114, F01007, doi: 10.1029/2008JF001088.

Zattin, M., Landuzzi, A., Picotti, V., and Zuffa, G.G., 2000, Discriminating between tectonic and sedimentary burial in a foredeep succession, Northern Apennines: Journal of the Geological Society, v. 157, p. 629–633.

Zattin, M., Picotti, V., and Zuffa, G.G., 2002, Fission track reconstruction of the front of the Northern Apennines thrust wedge and overlying Ligurian Unit: American Journal of Science, v. 302, p. 346–379, doi: 10.2475/ajs.302.4.346.

Zhang, P.Z., Molnar, P., and Downs, W.R., 2001, Increased sedimentation rates and grain sizes 2–4 Myr ago due to the influence of climate change on erosion rates: Nature, v. 410, p. 891–897, doi: 10.1038/35073504.

MANUSCRIPT RECEIVED 4 JANUARY 2010
REVISED MANUSCRIPT RECEIVED 24 FEBRUARY 2010
MANUSCRIPT ACCEPTED 25 FEBRUARY 2010

Printed in the USA